P-ISSN 1991-8941
E-ISSN 2706-6703
Vol. 19, No. 2 (2025)

Journal of University of Anbar for Pure Science
(JUAPS)

journal homepage: juaps.uoanbar.edu.iq

Open Access

Original Paper

Preparation of aluminum sulfate nanoparticles prepared by the green method and study of their effect on a poly(vinyl chloride) surface

Namaa Raad Attallah [1*], **Hameed Khalid Ali** [1], **Muthana Mohammad Sirhan** [1]

[1]Department of Chemistry, College of Education for Pure Science , University of Anbar, Ramadi, Iraq

ARTICLE INFO

Received: 04/03/2025
Accepted: 04/05/2025
Available online: 07/11/2025
December Issue
10.37652/juaps.2025.157929.1361

Cite @ JUAPS

Corresponding author
Namaa Raad Attallah
nam23u4019@uoanbar.edu.iq

ABSTRACT

In this study, aluminum sulfate nanoparticles (ASNPs) were prepared using *Ziziphus spina* leaf extract. Poly(vinyl chloride) (PVC) films with a thickness of 50 ± 5 µm were then prepared by the casting method after adding the nanomaterial at different concentrations (0.04, 0.02, 0.01, 0.005, and 0.0025)% to a PVC solution dissolved in tetrahydrofuran. The prepared aluminum sulfate nanoparticles were characterized using a scanning electron microscope (SEM), which showed a particle size of 60.01 nm, and X-ray diffraction (XRD), which indicated an average diameter of 9.74 nm. The optical fragmentation of the polymer films was then evaluated in the presence and absence of the nanomaterials. UV-visible spectroscopy at a wavelength of 278 nm was used after different irradiation periods (0, 20, 40, 80, 120, 160 hours) to calculate the photodissociation constant (Kd) of the polymeric films in the presence of the nanomaterial additive. The results showed that increasing the nanomaterial concentration led to a higher photodegradation rate of the polymer films compared to the films without the additive. Infrared spectroscopy was also used to calculate the absorption coefficient of the carbonyl group (Ico). The absorption coefficient of the carbonyl group (Ico) in PVC increased with both nanomaterial concentration and irradiation time, and this increase was directly proportional to irradiation time.

The molecular mass of the polymer, the degree of disintegration, and the numerical rate of polymer chain scission (S) were also calculated using a viscometer. With increasing additive concentration and irradiation time, the molecular weight decreased, while both the chain scission rate and the degree of disintegration increased. Based on these findings, further work is recommended to investigate the impact of aluminum sulfate nanoparticles on different types of polymeric surfaces to enhance their physical and chemical properties. In addition, exploring alternative green synthesis methods may improve particle size distribution and overall material efficiency.

Keywords: *Aluminum Sulfate, Nanoparticles, Nano, Photodegradation, PVC,*

1 INTRODUCTION

Nanotechnology is the science concerned with studying structures and molecules on the scale of 1-100 nanometers. The term “nano” is derived from Greek and refers to something extremely small, corresponding to one-billionth of a meter [1]. Nanotechnology is an advanced research field that enables the production of a wide class of materials, including nanoparticles with at least one dimension in the nanoscale range (less than 100 nm), which gives the material new behaviors and properties [2].

These unique properties enable new applications in chemistry, physics, and the life sciences, as well as in medicine, engineering, and electronics. Polymers are an excellent host material for nanoparticles used to enhance their electrical properties. Recent research has identified applications for aluminum sulfate nanoparticles as an adjuvant in water decontamination processes, improving process efficiency and promoting more effective

sequestration of impurities [3]. The importance of this material is not limited to environmental applications, but also extends to industrial processes, where it enhances the mechanical and thermal properties of the materials involved and improves the quality of the final products [4].

Aluminum sulfate nanostructures play an important role in the production of advanced materials, such as insulating and active compounds. Their nanoscale properties contribute to increased resistance to heat and corrosion, making them an ideal choice for improving the performance of mechanical components. In addition, aluminum sulfate nanostructures show high thermal stability, making them suitable for applications that require high temperatures. They can also catalyze chemical reactions, contributing to improved engineering materials and reduced production costs [5, 6].

Poly(vinyl chloride) (PVC) is one of the most important plastics and is used in many applications, including building materials, automobiles, electrical wire insulation, pipes, and medical materials. It is also used in the manufacture of thin films and plastic sheets for greenhouses. PVC is made up of small chemical units called phenyl chloride (CH_2=CHCl), a derivative of ethylene gas (CH_2=CH_2), in which a chlorine atom is substituted for a hydrogen atom. However, PVC is sensitive to UV and direct sunlight. When exposed to these rays, photocatalytic processes within its structure begin to release hydrochloric acid (HCl) molecules. This leads to gradual deterioration of its mechanical properties and a visible change in color, from green to orange, to coffee, and finally to black [7].

Photofragmentation occurs as a result of the separation of polymer molecules and their transformation into smaller units under the influence of photons, as well as a change in molecular structure. This includes non-reflective transformations such as hydrogen stripping from the same polymer molecule, the addition of atoms or molecules to the polymer molecule, and oxidation, which is the most important reaction in photofragmentation. Physical and chemical changes occur when the polymer is exposed to UV and visible light. The efficiency of the photofragmentation process depends on the presence of light-absorbing colored aggregates in the polymer chain, which initiate photochemical reactions that produce initiators. These reactions lead to polymer dissociation and excitation, which results in the removal of hydrogen atoms from the polymer molecule and the formation of alkyl free radicals [8].

2 MATERIALS AND METHODS

2.1 Preparation of plant extract

The leaves of *Ziziphus spina* were washed with distilled water and cleaned of impurities using a sieve. The leaves were then oven-dried and ground into a fine powder. The powder was characterized at the Desert Studies Centre at Anbar University. Then, 10 g of the powder was added to 400 mL of deionized water in a glass flask, and the mixture was boiled for 30 minutes. After cooling, the solution was filtered and stored in the refrigerator [9] for use in the preparation of aluminum sulfate nanoparticles, as shown in Figure 1.

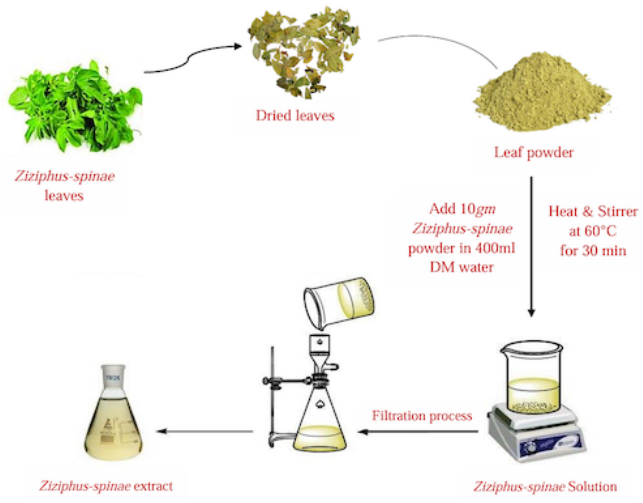

Fig. 1 Preparation steps *Ziziphus spina* Tree Leaves extract

2.2 Preparation of as nps

Twenty milliliters of aluminum sulfate solution (0.55 M) was added to 25 mL of Sidr extract with continuous stirring for 3 hours using a magnetic stirrer. The mixture was then left overnight to reach the desired consistency. After that, the mixture was dried at 150 °C and kept at 600 °C for 2 hours. The resulting material was ground into a fine powder and washed several times with deionized water and ethanol to remove impurities. Finally, the powder was dried at 70 °C in preparation for analysis and testing [10].

2.3 Preparation of poly(phenyl chloride)

Preparation of PVC was carried out by dissolving 6 g of the polymer in 100 mL of THF with continuous

stirring using a magnetic stirrer at room temperature to ensure homogenization for 1 hour [11].

2.4 Preparation of poly(vinyl chloride) membranes

To prepare PVC polymeric films, 0.04, 0.02, 0.01, 0.005, and 0.0025% aluminum sulphate nanoparticles were added to 5 mL of the PVC solution and mixed thoroughly before the mixture was poured onto glass slides. After ensuring that there were no bubbles, the mixture was allowed to dry for 15 min at room temperature. The films were then removed using a blade and forceps, and their thickness was set at 50 ± 5 µm. The films were cut into 3.5 × 1.5 cm pieces suitable for UV-Vis and FT-IR measurement cells.

2.5 Irradiation of the prepared membranes

The prepared membranes were irradiated using an 18 W lamp with a wavelength of 365 nm. The samples were arranged to ensure uniform exposure, and they were subjected to irradiation for specific periods (0, 40, 80, 120, 160 hours), as shown in Figure 2.

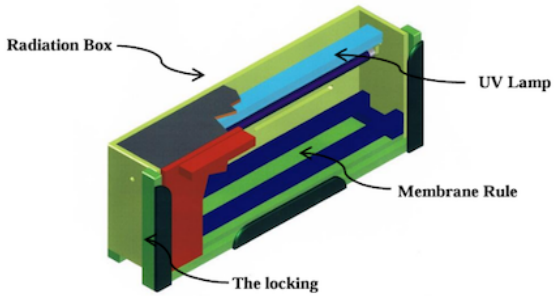

Fig. 2 Diagram showing the parts of the irradiator used in the study

2.6 Methods for monitoring the photodegradation of poly(vinyl chloride) membranes

2.6.1 Infrared spectroscopy

An infrared spectrometer was used to analyze PVC membranes before and after irradiation in the range of 4000-600 cm^{-1} to monitor the effect of irradiation on the material. The absorption band of the carbonyl group (C=O) at 1774 cm^{-1} was used to calculate the carbonyl growth coefficient (ICO) by applying the beam coefficient equation.

$$I_{(s)} = \frac{A_{(s)}}{A_{(R)}} \tag{1}$$

where
$I_{(s)}$ - the growth coefficient of the group under study.
$A_{(s)}$ - the absorbency of the group under study.
$A_{(R)}$ - the absorbance of the reference peak.

2.6.2 Uv-vis spectroscopy

A UV-Vis instrument was used to measure the absorbance of the polymeric films over a wavelength range of 200-600 nm. This measurement was used to assess changes in the films as a result of irradiation and to calculate the dissociation rate constant (Kd) during the photo-oxidation process of these membranes. Kd was calculated using first-order kinetics, as shown in Equation (2) below.

$$\ln(\ln(a-x)) = \ln(\ln(a)) - K_d t \tag{2}$$

where
a: Nanomaterial concentration before irradiation.
x: Nanomaterial concentration after time t of irradiation.
t: Irradiation time in seconds.

To confirm that the reaction follows first-order kinetics, the relationship between $\ln(a-x)$ and irradiation time (t) is plotted. When a straight line is obtained, this indicates first-order behavior, and the slope of the line represents the dissociation constant ($-K_d$) [12].

2.6.3 Viscosity measurement

The viscosity method was used to determine the molecular weight and fractionation rate of the polymer films. The analysis was based on the Mark-Houwink equation, which relates viscosity properties to the molecular weight of the polymer. Using this equation, the molecular weight of the polymer was determined from viscosity measurements. The degree of fractionation (α) was then calculated using the following relationship [13, 14].

$$\alpha = \frac{1}{P_t} - \frac{1}{P_0} \tag{3}$$

The numerical rate of cutting the S series is calculated from equation (4).

$$S = \frac{M_{v0}}{M_{vt}} - 1 \tag{4}$$

2.6.4 Optical microscope

An optical microscope was used to image PVC membranes and aluminum sulfate nanoparticle-polymer composites before and after irradiation, in order to observe and evaluate surface changes resulting from UV exposure.

3 RESULTS AND DISCUSSION

The study results demonstrated the green synthesis of aluminum sulfate nanoparticles, achieving a good size distribution and uniform morphology. The nanoparticles showed clear potential for modifying the surface properties of PVC, highlighting the effectiveness of eco-friendly methods in enhancing polymer performance.

3.1 Gas chromatography-mass spectrometry (gc-ms)

The GC-MS technique combines gas chromatography and mass spectrometry to analyze organic chemical compounds, where the components of a mixture are first separated and then analyzed in detail [15]. Using this technique, three compounds were detected in Sidr *(Ziziphus spina)* leaf extract, most notably hexadecanoic acid, which showed the highest peak at 63.092 min. Other compounds, such as octadecanoic acid, appeared with lower peaks. The retention times of the compounds varied, indicating the diversity of the chemical composition of the extract. The results confirmed that the extract is rich in saturated and unsaturated fatty acids, which have nutritional, medical, and cosmetic benefits. These compounds contribute to antioxidant and anti-inflammatory properties, as shown in Table 1 and Figure 3.

Table 1 GC-MS analysis of *Ziziphus spina* leaves extract

(Peak)	(RT) (min)	(%Area)	Discovered compound	Molecular formula	M.WT (g/mol)	(Qual)
1	57.457	19.02	n-Hexadecanoic acid	$C_{16}H_{32}O_2$	256.42	99
			n-Hexadecanoic acid			97
			n-Hexadecanoic acid			97
2	63.058	38.53	9-Octadecenoic acid, (E)-	$C_{18}H_{34}O_2$	282.46	99
			Oleic Acid			99
			9-Octadecenoic acid (Z)-			99
3	63.092	42.45	9-Octadecenoic acid, (E)-	$C_{18}H_{34}O_2$	282.46	99
			Oleic Acid			99
			6-octadecenoic acid			99

3.2 X-ray diffraction

Figure 4 shows the X-ray diffraction results of the prepared aluminum sulfate nanoparticles compared to the standard pattern (JCPDS No. 00-043-0030). The main peaks appear at 2θ angles of 14.70°, 25.54°, 27.46°, 45.80°, 53.15°, and 55.06°, indicating the crystalline structure of the material. The average size of the nanoparticles was calculated using the Debye–Scherrer equation, with an average size of about 9.74 nm.

3.3 Scanning electron microscopy

The SEM technique relies on directing a beam of electrons toward the area to be examined, where the electrons interact with surface atoms. This interaction produces three types of signals, including secondary electrons, backscattered electrons, and X-rays.

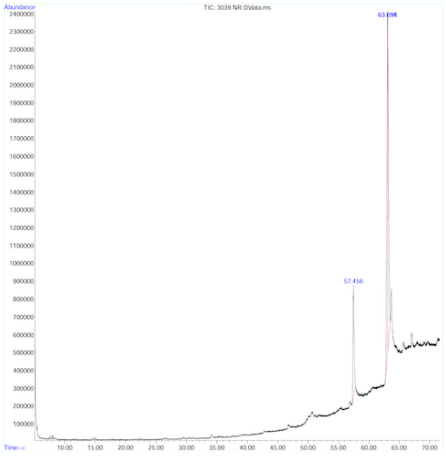

Fig. 3 GC-MS analysis of *Ziziphus spina* leaves extract

The technique allows very high magnification, ranging from 50× to 200,000×, which enables analysis and identification of surface details with high precision [16].

The analysis of aluminum sulfate nanoparticles obtained from *Ziziphus spina* leaf extract indicates that these particles have an irregular shape, with sizes ranging from 60.01 to 63.89 nm, as shown in Figure 5. The images also reveal the presence of small agglomerates in the particle structure, which may be due to the nature of the material itself or to the preparation method.

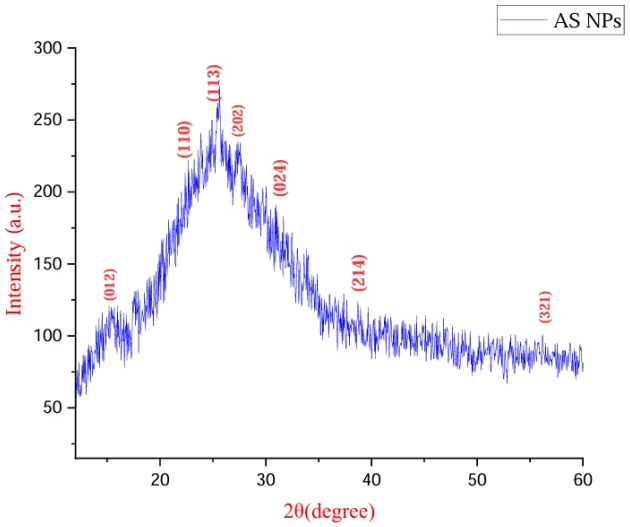

Fig. 4 XRD pattern of aluminum sulfate nanoparticles

These results are consistent with previous work that indicated a successful production of nanoparticles with uniform distribution using green synthesis approaches [10]. Minor differences in particle size and morphology may be due to differences in synthesis conditions and precursor concentrations.

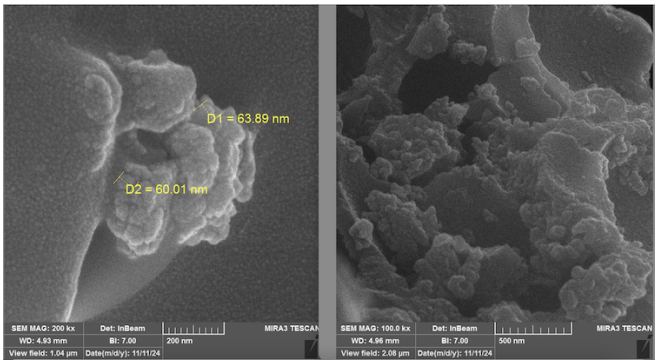

Fig. 5 SEM images of aluminum sulfate NPs at a magnification of 200,000x showing nanoparticles with irregular morphology and an average size ranging between 60 and 64 nm, with slight agglomerations observed across the sample surface

3.4 Photofragmentation of poly(vinyl chloride)

The photofragmentation of PVC films with a thickness of 50 ± 5 µm, both pure and containing different concentrations of aluminum sulfate nanoparticles (AS NPs), was monitored to evaluate the effect of increasing AS NP concentration on polymer dissociation at different irradiation times. This assessment was performed using UV-Vis, FT-IR, viscometry, and light microscopy measurements.

3.5 Uv-visible spectroscopy

UV-Vis spectroscopy was used to study the optical properties of aluminum sulfate nanoparticles (ASNPs). The spectra of these samples were measured within a wavelength range of 200-600 nm at room temperature [17]. This analysis was also used to monitor the effect of AS NPs on the fragmentation of PVC films during UV exposure. When pure PVC films and PVC films containing different percentages of AS NPs were exposed to UV light, a yellow discoloration of the films was observed as a result of polymer degradation. These results are summarized in Table 2, where the photodegradation rate constant (K_d) was calculated based on absorbance values obtained after different irradiation times. The results showed that film absorbance depends on both irradiation time and the concentration of added AS NPs.

From Table 2, the absorbance values of pure PVC films are directly proportional to irradiation time. The absorbance was 0.205 before irradiation and reached 0.373 after 160 hours of irradiation. When aluminum sulfate nanoparticles added at different concentrations, the absorbance increased further compared to the pure polymer. For example, at an irradiation time of 120 hours, the absorbance of the pure polymer was 0.315, which increased to 0.361 with 0.0025% ASNPs and reached 0.622 at a concentration of 0.04%.

Table 2 Absorbancy value of PVC films

Chip type / Irradiation Time (hrs.)	Absorbance (A_t)				
	0.0	**40**	**80**	**120**	**160**
PVC	0.205	0.244	0.280	0.315	0.373
PVC + 0.0025% Nano- Aluminum sulfate	0.207	0.256	0.321	0.361	0.415
PVC+ 0.005 % Nano- Aluminum sulfate	0.209	0.280	0.367	0.434	0.492
PVC + 0.01 % Nano- Aluminum sulfate	0.210	0.302	0.395	0.513	0.563
PVC + 0.02 % Nano- Aluminum sulfate	0.211	0.354	0.450	0.558	0.607
PVC + 0.04 % Nano- Aluminum sulfate	0.212	0.409	0.514	0.622	0.699

Polymeric films prepared with a thickness of 50 ± 5 µm and containing ASNPs showed an increase in absorbance with increasing nanomaterial concentration, due to the presence of more active aggregates, as indicated in Figures 6 to 8. To calculate the photodissociation constant (K_d), the relationship between $\ln(A_0 - A_\infty)$ and irradiation time was plotted, and the result was a straight line. This indicates that the photoreaction is first order, as shown in Figures 9 to 10.

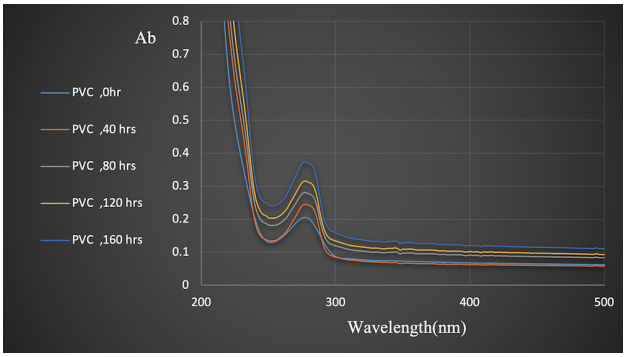

Fig. 6 Change in UV-visible spectrum of poly(vinyl chloride) films without additives

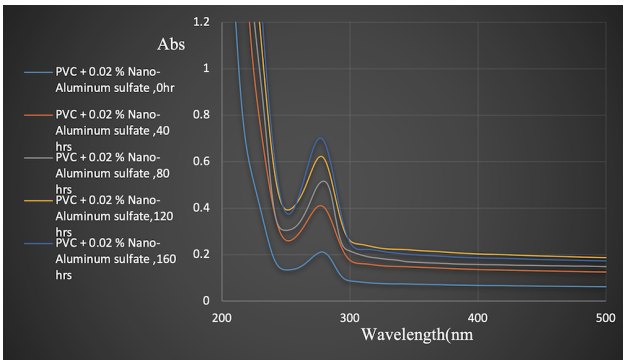

Fig. 7 Change in UV-visible spectrum of poly(vinyl chloride) films containing 0.02% concentration of aluminum sulfate nanoparticles

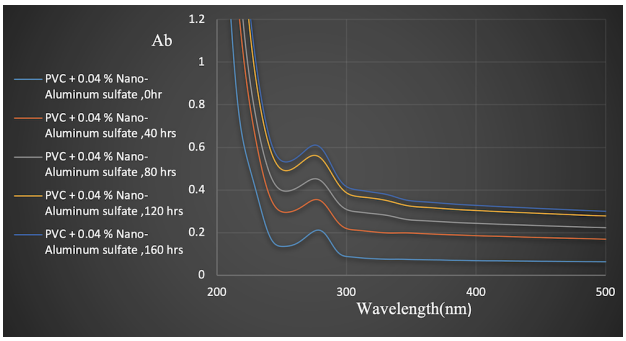

Fig. 8 Change in UV-visible spectrum of poly(vinyl chloride) films containing 0.04% concentration of aluminum sulfate nanocomposite

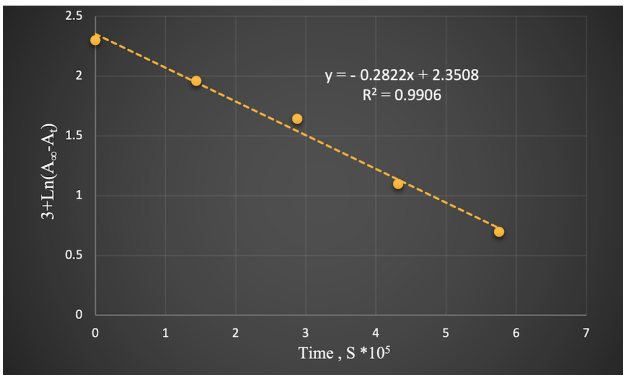

Fig. 9 Relationship between the natural logarithm of the absorbance of aluminum sulfate nanocomposites at a concentration of 0.02% in poly(vinyl chloride) films

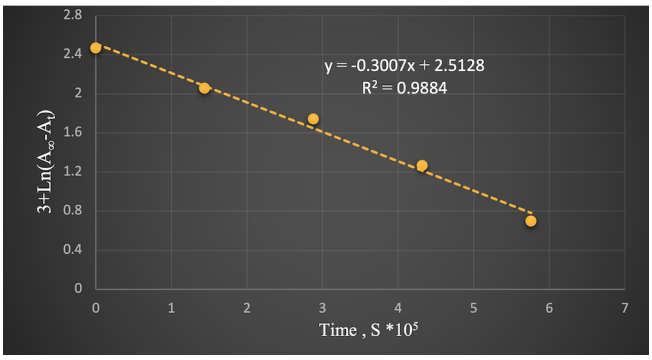

Fig. 10 Relationship between the natural logarithm of the absorbance of aluminum sulfate nanoparticles at a concentration of 0.04% in poly(vinyl chloride)

By calculating the slope of the straight line from the above figures, the photodissociation speed constant (K_d) was obtained for aluminum sulfate nanoparticles added to PVC at the stated concentrations. The results show that the photodissociation speed constant is directly proportional to the concentration of the nanomaterial added to the polymer, as shown in Table 3. This indicates that aluminum sulfate nanoparticles increase the rate of light-induced interaction with the polymer.

Table 3 Absorbancy value of PVC films

Concentration %	K_d **(Sec.)**$^{-1} \times 10^{-5}$
PVC + 0.0025% Nano-Aluminum sulfate	0.192
PVC+ 0.005% Nano-Aluminum sulfate	0.233
PVC + 0.01% Nano-Aluminum sulfate	0.270
PVC + 0.02% Nano-Aluminum sulfate	0.282
PVC + 0.04% Nano-Aluminum sulfate	0.300

3.6 Infrared spectroscopy

The photodegradation of pure PVC films containing different concentrations of AS NPs was studied using Fourier-transform infrared (FT-IR) spectroscopy in the range of 600-4000 cm$_{-1}$. The analysis focused on the absorption band of the carbonyl group (C=O), which is generated by the impact of photons in the presence of oxygen and appears at 1774 cm$_{-1}$. In this process, oxygen acts as a catalyst, and AS NPs act as a catalyst for disintegration [18]. The FT-IR spectra of the poly(vinyl chloride) films, both pure and those containing aluminum sulfate nanoparticles, showed significant changes after UV irradiation. A notable absorption peak appeared around 1774 cm$_{-1}$, corresponding to the stretching vibration of the carbonyl (C=O) group. This peak increased

with both irradiation time and nanomaterial concentration, indicating enhanced photo-oxidative degradation. The presence of characteristic functional groups related to aluminum sulfate was also confirmed, with distinct absorption bands observed near 1100 cm_{-1} and 3500 cm_{-1}, supporting successful incorporation of the nanoparticles into the polymer matrix.

Monitoring carbonyl band growth is an important tool for evaluating the chemical behavior of polymeric films, with the highest values observed at high AS NP concentration. The carbonyl growth coefficient was calculated using the baseline method. After exposing pure PVC films with a thickness of 50 ± 5 µm to different irradiation durations, FT-IR measurements showed changes in the spectra before and after irradiation. Figure 11 shows the spectrum of pure PVC before irradiation, while Figure 12 shows the spectrum after 160 hours of irradiation. A clear change in the carbonyl group band is observed due to UV exposure.

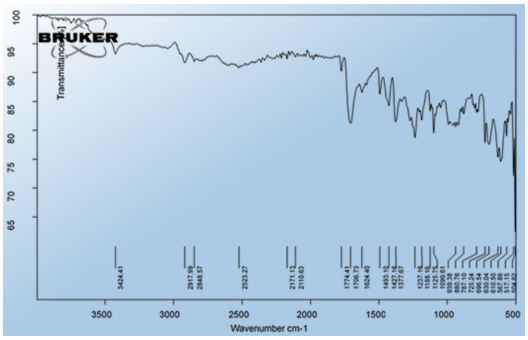

Fig. 11 Infrared spectrum of a poly(vinyl chloride) film without additives before irradiation.

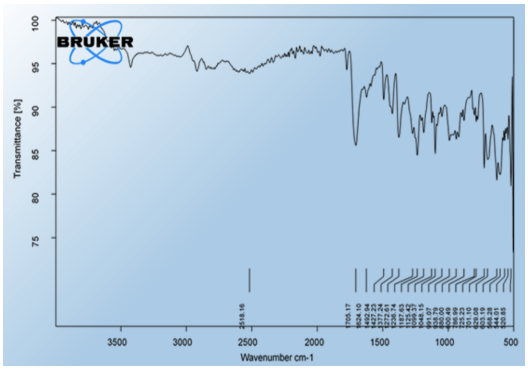

Fig. 12 Infrared spectrum of an additive-free poly(vinyl chloride) film with an irradiation time of 160 hours.

For the PVC film containing 0.04% aluminum nanosulfate, the change can be observed in Figure 13, which shows the infrared spectrum of the PVC film with 0.04% aluminum nanosulfate after 160 hours of irradiation.

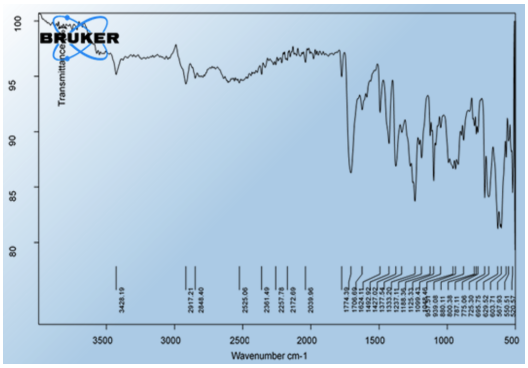

Fig. 13 Infrared spectrum of a poly(vinyl chloride) film containing 0.04% concentration of aluminum sulfate nanoparticles with an irradiation time of 160 hours

Table 4 Carbonyl adsorption coefficient (ICO) values with irradiation time for poly(vinyl chloride) containing different concentrations of aluminum sulfate nanocomposites

Irradiation time(hrs.) / Wt. % of Addition	I_{CO} 0.0	40	80	120	160
PVC	1.011	1.018	1.111	1.213	1.281
PVC + 0.0025 % Nano-Aluminum sulfate	1.061	1.101	1.188	1.305	1.401
PVC + 0.005% Nano-Aluminum sulfate	1.113	1.215	1.316	1.408	1.556
PVC + 0.01 % Nano-Aluminum sulfate	1.198	1.293	1.401	1.518	1.674
PVC + 0.02 % Nano-Aluminum sulfate	1.213	1.374	1.542	1.667	1.791
PVC + 0.04 % Nano-Aluminum sulfate	1.245	1.489	1.653	1.823	1.896

When comparing the infrared spectrum of pure PVC film with that of the film containing 0.04% AS NPs after 160 hours of irradiation, the change in the carbonyl band peaks was greater in the film containing AS NPs than in the pure film. This indicates that aluminum sulfate nanoparticles promote the photodegradation of PVC. The carbonyl group absorption coefficient values were calculated for the pure film and for films containing different concentrations of AS NPs, as shown in Table 4.

From Figures 14 and 15, the speed of photo-oxidative degradation increases with both irradiation time and the concentration of aluminum nanosulfate added to the PVC films. This relationship is directly proportional. The increase in degradation rate is associated with increased absorbance of the polymer films to UV light during

irradiation, along with higher values of the carbonyl group absorption coefficient, which leads to an increase in the speed of photo-oxidative degradation of the polymer films.

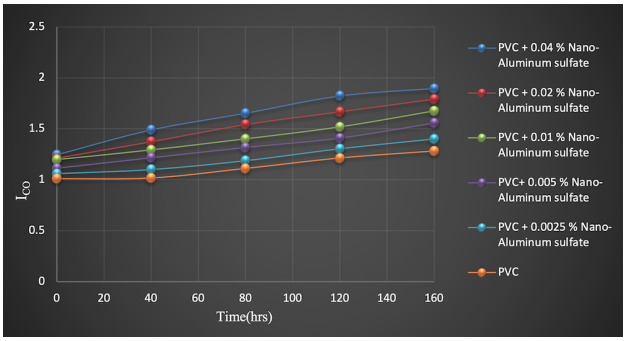

Fig. 14 Relationship between carbonyl absorption coefficient and irradiation time for the results in Table 4

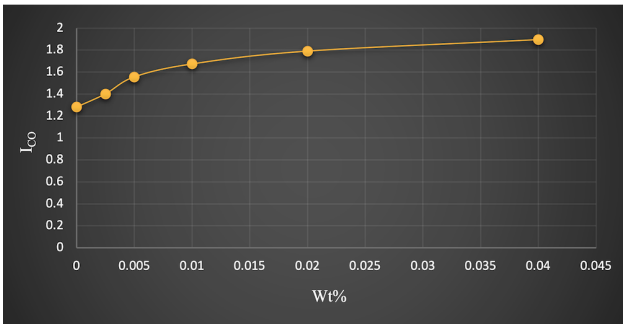

Fig. 15 Change in carbonyl adsorption coefficient with aluminum sulfate nanocomposites concentration for poly(vinyl chloride) films (160) hours

The findings of this study highlight the critical role of aluminum sulfate nanoparticles in promoting UV-induced photodegradation of PVC films. These results indicate a possible pathway for developing environmentally friendly polymeric materials with enhanced degradation characteristics suitable for industrial and environmental applications.

3.7 Viscosity measurement

The photodegradation process of pure PVC films containing different concentrations of aluminum nanosulfate was evaluated by calculating the average viscous molecular weight of the films before and after irradiation. Measurements showed that the intrinsic viscosity and viscous molecular weight of pure PVC films are inversely proportional to irradiation time. This decrease is attributed to increased polymer chain disintegration and crosslinking, which result in lower molecular weight. A similar effect was observed in films containing aluminum sulfate nanoparticles (0.005%), where the results were compared with those of pure films. Tables 5 and 6 show the calculated viscous molecular weight values of pure PVC, confirming this relationship.

The calculated values in Table 5 show that polymeric films containing 0.005% nanoparticulate aluminum sulfate behave similarly to pure polymeric films, but with a greater effect. The presence of nanoscale aluminum sulfate in PVC increases the rate of viscous molecular weight reduction compared to pure polymeric films, as shown in Figure 16. The results indicated that aluminum sulfate nanocomposites accelerate the decrease in viscous molecular weight (Mv) with irradiation time compared to pure polymer films, consistent with their role as photodegradation accelerators. The rate of decrease in Mv is large at the beginning of irradiation due to the breaking of weak bonds and then slows as irradiation continues. When these bonds are randomly distributed along the polymer chain, the rate of change in Mv (dMv/dt) is proportional to the square of the viscous molecular weight, $(Mv)_2$, at a given time.

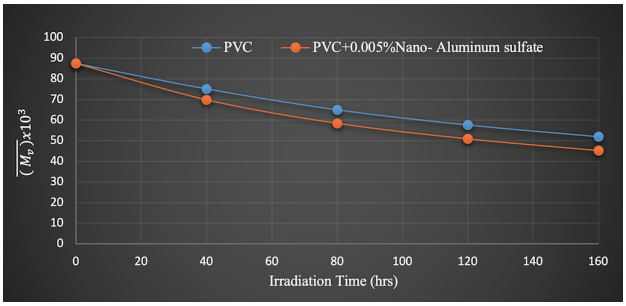

Fig. 16 Relationship of average viscous molecular weight with irradiation time for poly(vinyl chloride) films With and without (0.005%) concentration of aluminum sulfate nanoparticles

From the values of the numerical rate of polymer chain scission, *S*, calculated using the equation in Tables 5 and 6, and its relationship with irradiation time, it is shown in Figure 17 that the relationship is linear. This behavior confirms the presence of weak bonds that are randomly distributed along the length of the polymer chain.

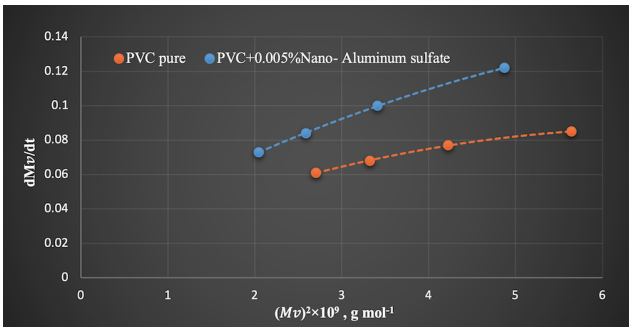

Fig. 17 Relationship between the speed of decrease in molecular weight rate (dMv/dt) and the square of the viscous molecular weight rate for poly(vinyl chloride) films In the presence and absence of 0.005% concentration) of aluminum sulfate nanoparticles

Figures 18 and 19 confirm the dissolution of pure poly(vinyl chloride) films and films containing different concentrations of nanoscale aluminum sulfate in a random manner.

From Tables 5 and 6, the values of the degree of disintegration (α) of poly(vinyl chloride) films containing 0.005% nanomaterial are higher than those of pure polymer films. This indicates that aluminum nanosulfate accelerates the disintegration process through photo-oxidation of the polymer. The adopted green synthesis method offers several advantages, including simplicity, low cost, and reduced environmental impact. However, achieving complete uniformity in nanoparticle size and preventing minor agglomeration remain challenges that should be addressed in future work to further optimize the synthesis process.

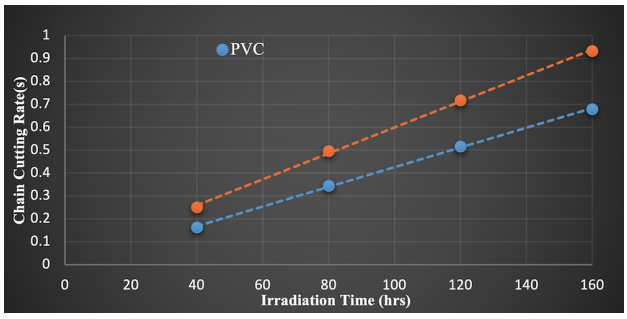

Fig. 18 Relationship of the numerical rate of chain cutting with irradiation time for poly(vinyl chloride) films in the presence and absence of 0.005% concentration of aluminum sulfate nanoparticles

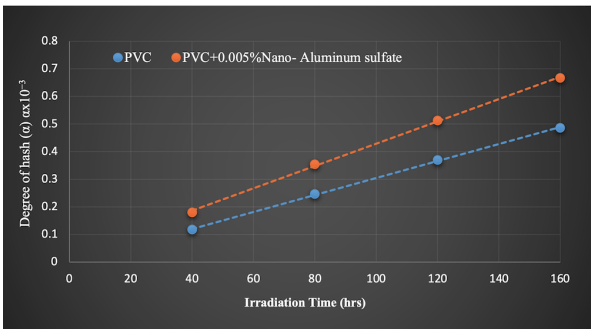

Fig. 19 Relationship of the degree of fractionation with irradiation time for poly(vinyl chloride) films in the presence and absence of (0.005%) concentration of aluminum sulfate nanoparticles

3.8 pvc light microscopy

Photomicrographs of pure PVC films containing 0.01% aluminum sulfate nanoparticles show that the film surface is affected by UV energy, with a clear difference before and after irradiation. After exposure to UV light for 160 hours, deformation of the polymer film surface was observed due to the interaction between light and the added nanomaterial, which accelerates the disintegration process, as illustrated in Figures 20 and 21.

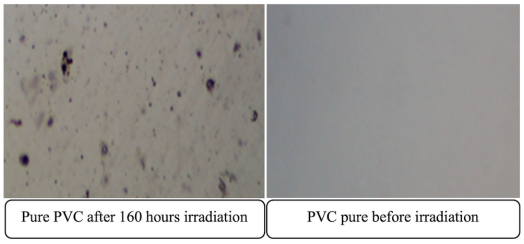

Fig. 20 Micrographs of the surface of the pure poly(vinyl chloride) polymer before and after irradiation for 160 hours.

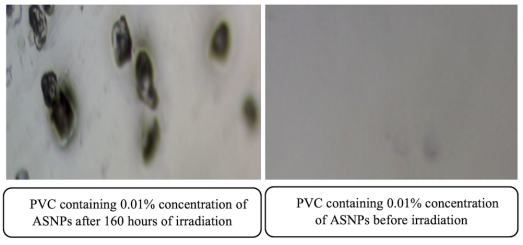

Fig. 21 Micrographs of a poly(vinyl chloride) surface containing 0.01% concentration of aluminum sulfate nanocomposite before and after irradiation for 160 hours.

Table 5 Calculated values from viscous molecular weight measurements of poly(vinyl chloride) films Pure

Irradiation time (hours)	$\bar{M}_v \times 10^3$	$(M_v)^2 \times 10^9$	$\frac{dM_v}{dt} = \frac{M_{v0}-M_{vt}}{t}$	Degree of polymerization (P)	$\frac{1}{P} \times 10^{-4}$	Degree of fractionation $a \times 10^{-3}$	Chain scission rate (S)
0	87.442	7.646	∞	1399.072	7.147	0.0	0.0
40	75.124	5.643	0.085	1201.984	8.319	0.117	0.163
80	65.001	4.225	0.077	1040.016	9.615	0.246	0.344
120	57.661	3.324	0.068	922.576	10.839	0.369	0.516
160	52.010	2.705	0.061	832.160	12.016	0.486	0.679

Table 6 Calculated values from viscous molecular weight measurements of poly(vinyl chloride) films containing 0.005% concentration of aluminum sulfate nanoparticles

Irradiation time (hours)	$\bar{M}_v \times 10^3$	$(M_v)^2 \times 10^9$	$\frac{dM_v}{dt} = \frac{M_{v0}-M_{vt}}{t}$	Degree of polymerization (P)	$\frac{1}{P} \times 10^{-4}$	Degree of fractionation $a \times 10^{-3}$	Chain scission rate (S)
0	87.442	7.646	∞	1399.072	7.147	0.0	0.0
40	69.801	4.872	0.122	1116.816	8.954	0.180	0.251
80	58.423	3.413	0.100	934.768	10.697	0.355	0.496
120	50.890	2.589	0.084	814.240	12.281	0.513	0.717
160	45.211	2.044	0.073	723.376	13.824	0.667	0.933

4 CONCLUSION

Aluminum sulfate nanocomposites were prepared using Sidr leaf extract, and their synthesis was confirmed by scanning electron microscopy (SEM) and X-ray diffraction (XRD). The effect of these nanocomposites on the photocatalytic fractionation process of PVC films and the resulting changes was studied. XRD analysis was used to investigate the structural and chemical properties of the resulting composites. The behavior of aluminum sulfate nanoparticles as photodegradation accelerators in polymers was confirmed, as the disintegration speed constant (Ka) and the carbonyl group growth coefficient were found to be directly proportional to AS NP concentration and irradiation time. Aluminum sulfate nanoparticles increase light absorption, which supports the use of PVC/AS NPs systems to reduce environmental pollution. Our recommendation is to refine the synthesis process parameters to achieve better nanoparticle size control and reduce aggregation issues. Further studies should investigate the effect of aluminum sulfate nanoparticles on different types of polymeric materials to expand their potential applications in sustainable industries. Our recommendation is screening for bacterial vaginosis in women with a history of miscarriage to help mitigate the risk of spontaneous abortion, particularly in early pregnancy.

FUNDING SOURCE

No funds received.

DATA AVAILABILITY

N/A

DECLARATIONS

Conflict of interest

The authors declare that they have no known competing financial interests.

Consent to publish

All authors consent to the publication of this work.

Ethical approval

N/A

REFERENCES

[1] Bayda S, Adeel M, Tuccinardi T, Cordani M, Rizzolio F. The History of Nanoscience and Nanotechnology: From Chemical–Physical Applications to Nanomedicine. Molecules. 2019;25(1):112. 10.3390/molecules25010112

[2] Saleh TA. Nanomaterials: Classification, properties, and environmental toxicities. Environmental Technology & Innovation. 2020;20:101067. 10.1016/j.eti.2020.101067

[3] Klein T. Wet chemical synthesis of nano and submicron Al particles for the preparation of Ni and Ru aluminides. Saarländische Universitäts-und Landesbibliothek. 2020

[4] Liew PJ, Yap CY, Wang J, Zhou T, Yan J. Surface modification and functionalization by electrical discharge coating: a comprehensive review. International Journal of Extreme Manufacturing. 2020;2(1):012004. 10.1088/2631-7990/ab7332

[5] Tahraoui H, Toumi S, Boudoukhani M, Touzout N, Sid ANEH, Amrane A, et al. Evaluating the Effectiveness of Coagulation–Flocculation Treatment Using Aluminum Sulfate on a Polluted Surface Water Source: A Year-Long Study. Water. 2024;16(3):400. 10.3390/w16030400

[6] Jafar-Tafreshi M, Bustanafruz F, Fazli M. Studies on thermal decomposition of aluminium sulfate to produce alumina nano structure. Journal of Nanostructures. 2012;2(4):463-8

[7] Shihab O, Ali H, Abdo N. Induced Photodegradation of Poly (Vinyl Chloride) by using Cobalt (II) – Complex [Co (C20H26N6O4)]Cl2. 2015;9:146-58. 10.37652/juaps.2015.175937

[8] Nguyen T, Martin JW, Byrd E, Embree E, Embree E. Effects of spectral UV on degradation of acrylic-urethane coatings. In: Proceedings of the 80th Annual Meeting of the program of the FSCT, Federation of Societies for Coatings Technology, October30-November. vol. 1; 2002. p. 2002

[9] hassan r, Ali H, Sirhan M. Preparing sulfur nanoparticles and determining their effect on the photodegradation of polycarbonates. Journal of University of Anbar for Pure Science. 2024;18(2):112–122. 10.37652/juaps.2024.148119.1223

[10] Garvasis J, Prasad AR, Shamsheera KO, Jaseela PK, Joseph A. Efficient removal of Congo red from aqueous solutions using phytogenic aluminum sulfate nano coagulant. Materials Chemistry and Physics. 2020;251:123040. 10.1016/j.matchemphys.2020.123040

[11] Deshmukh K, Joshi GM. Thermo-mechanical properties of poly (vinyl chloride)/graphene oxide as high performance nanocomposites. Polymer Testing. 2014;34:211–219. 10.1016/j.polymertesting.2014.01.015

[12] F Al-Rawi M, Mishaal Mohammed A, K AL-Duliami H. Studying the Effect of Magnesium Oxide Nanoparticles Prepared on the Surface of Poly Methyl Methacrylate. Baghdad Science Journal. 2020;17(2). 10.21123/bsj.2020.17.2(si).0642

[13] Wang J, Huang H, Huang X. Molecular weight and the Mark-Houwink relation for ultra-high molecular weight charged polyacrylamide determined using automatic batch mode multi-angle light scattering. Journal of Applied Polymer Science. 2016;133(31). 10.1002/app.43748

[14] Gopalakrishnan K, Ramesh C, Ragunathan V, Thamilselvan M. Antibacterial activity of Cu2O nanoparticles on E. coli synthesized from Tridax procumbens leaf extract and surface coating with polyaniline. Digest Journal of Nanomaterials and Biostructures. 2012;7(2):833-9

[15] Hastie C, Thompson A, Perkins M, Langford VS, Eddleston M, Homer NZ. Selected Ion Flow Tube-Mass Spectrometry (SIFT-MS) as an Alternative to Gas Chromatography/Mass Spectrometry (GC/MS) for the Analysis of Cyclohexanone and Cyclohexanol in Plasma. ACS Omega. 2021;6(48):32818–32822. 10.1021/acsomega.1c03827

[16] Lin Y, Zhou M, Tai X, Li H, Han X, Yu J. Analytical transmission electron microscopy for emerging advanced materials. Matter. 2021;4(7):2309-39

[17] Cimitan S, Albonetti S, Forni L, Peri F, Lazzari D. Solvothermal synthesis and properties control of doped ZnO nanoparticles. Journal of Colloid and Interface Science. 2009;329(1):73–80. 10.1016/j.jcis.2008.09.060

[18] Li X, Cheng S, Deng S, Wei X, Zhu J, Chen Q. Direct Observation of the Layer-by-Layer Growth of ZnO Nanopillar by In situ High Resolution Transmission Electron Microscopy. Scientific Reports. 2017;7(1). 10.1038/srep40911

How to cite this article

Attallah NR, Ali HK, Sirhan MM. Preparation of aluminum sulfate nanoparticles prepared by the green method and study of their effect on poly(vinyl chloride) surface. Journal of University of Anbar for Pure Science. 2025; 19(2):73-83. doi:10.37652/juaps.2025.157929.1361